*applied sciences*

MDPI

*Article*

# Forecasting of NOx Emissions of Diesel LHD Vehicles in Underground Mines—An ANN-Based Regression Approach

**Aleksandra Banasiewicz [1], Forougholsadat Moosavi [1], Michalina Kotyla [1], Paweł Śliwiński [2], Pavlo Krot [1,*], Jacek Wodecki [1] and Radosław Zimroz [1]**

1 Faculty of Geoengineering, Mining and Geology, Wroclaw University of Science and Technology, Na Grobli 15, 50-421 Wroclaw, Poland; aleksandra.banasiewicz@pwr.edu.pl (A.B.); forougholsadat.moosavi@pwr.edu.pl (F.M.); michalina.kotyla@pwr.edu.pl (M.K.); jacek.wodecki@pwr.edu.pl (J.W.); radoslaw.zimroz@pwr.edu.pl (R.Z.)
2 KGHM Polska Miedz S.A, ul. Marii Skłodowskiej-Curie 48, 59-301 Lubin, Poland; pawel.sliwinski@kghm.com
* Correspondence: pavlo.krot@pwr.edu.pl

**Abstract:** An approach based on an artificial neural network (ANN) for the prediction of NOx emissions from underground load–haul–dumping (LHD) vehicles powered by diesel engines is proposed. A Feed-Forward Neural Network, the Multi-Layer Perceptron (MLP), is used to establish a nonlinear relationship between input and output layers. The predicted values of NOx emissions have less than 15% error compared to the real values measured by the LHD onboard monitoring system by the standard sensor. This is considered quite good efficiency for dynamic behaviour prediction of extremely complex systems. The achieved accuracy of NOx prediction allows the application of the ANN-based "soft sensor" in environmental impact estimation and ventilation system demand planning, which depends on the number of working LHDs in the underground mine. The proposed solution to model NOx concentrations from mining machines will help to provide a better understanding of the atmosphere of the working environment and will also contribute to improving the safety of underground crews.

**Keywords:** NOx emission prediction; artificial neural network; LHD vehicles; underground mine; safety; ventilation

check for updates

**Citation:** Banasiewicz, A.; Moosavi, F.; Kotyla, M.; Śliwiński, P.; Krot, P.; Wodecki, J.; Zimroz, R. Forecasting of NOx Emissions of Diesel LHD Vehicles in Underground Mines—An ANN-Based Regression Approach. *Appl. Sci.* **2023**, *13*, 9965. https://doi.org/10.3390/app13179965

Academic Editor: Johannes Schwank

Received: 31 July 2023
Revised: 23 August 2023
Accepted: 2 September 2023
Published: 4 September 2023



## 1. Introduction

In underground mining, the movement of crews is realized by wheeled vehicles. This is due to the long distances between the shaft and the mining sections where the underground crews work. In Polish copper ore mines, almost all vehicles are powered by diesel engines [1,2]. In addition to vehicles for transporting people, the largest part of the mine's fleet consists of trucks and loaders, which transport the material to be excavated. Underground crews face mobility problems due to long distances of up to several kilometres. One of the major ventilation problems is the transport of fresh air to distant worksites. In the deep mines, apart from an increase in air temperature along with the transport distance, air pollution also increases.

According to Dong et al. [3], underground mines face many natural hazards that affect air quality. One of the most important hazards affecting air quality is the gas hazard. The most dangerous of these to the human body are carbon monoxide (CO), methane ($CH_4$), hydrogen sulphide ($H_2S$), and nitrogen oxides (NOx) [4–7]. Gases such as $H_2S$ or $CH_4$ are gases that are of natural sources. NOx and CO are gases whose presence in mine air is generated mainly by technological processes.

Diesel machinery is considered the source of the highest amount of nitrogen oxides in an underground mine [8]. The NOx emissions from vehicles have been analysed to develop analytical tools based on ANN for their prediction. A type of Feed-Forward Neural Network, the Multi-Layer Perceptron (MLP), has been used to develop a nonlinear relationship between input and output layers for predicting NOx emissions from load–haul–dumping (LHD) vehicles in underground mines.

The obtained NOx prediction accuracy allows the use of the MLP "soft-sensor" for estimating the environmental impact and to plan the ventilation system demand depending on the number of operating LHDs in the underground mine. The measurement data were analysed from the SYNAPSA system mounted on the LHD machine. This system monitors various parameters, such as engine speed, engine acceleration, fuel consumption, oil temperature, and oil pressure, some of which also measure NOx concentrations. Based on these data, a prediction model was created using the MLP network, which is often used to forecast gas emissions [9,10].

To ensure the safety of underground mining crews, it is crucial to have accurate information about the emissions of harmful compounds from mining machinery. The prediction model developed in this study is a valuable tool that can be used to estimate the emissions values of mining machinery that does not have a nitrogen oxide sensor installed. Using the prediction model to estimate emissions values, mining companies can take appropriate measures to ensure the safety of their workers and the surrounding environment.

## 2. State of the Art

Ventilation in underground mines can be a costly and complex process, as it depends on factors such as the mining technology and the geometry of the mine. Additionally, local air quality can fluctuate, which poses a risk to miners.

Ensuring the safety of underground mining crews is of utmost importance in mining operations. This is reflected in various regulations that impose restrictions on human work in excavations where working conditions may pose a risk to workers' health or safety [11–15]. Examples of such regulations include legal acts that limit the temperature or the concentration of harmful substances in the workplace. These acts also define different types of natural hazards that may affect workers in underground mines [16].

Adhering to these regulations and taking appropriate measures to mitigate risks is crucial for maintaining a safe work environment for underground mining crews. As mining operations move away from the main underground excavations and intake shafts, the risk of natural hazards in underground mines increases [17–19]. Of these hazards, the atmospheric and gas hazards pose the greatest danger. Harmful gases can enter the mine atmosphere naturally, such as methane and hydrogen sulphide, or as a result of technological processes, including carbon monoxide and nitrogen oxides. In recent years, scientists have been analysing the impact of nitrogen oxides (NOx) in underground mines, as they are one of the most harmful gases present. In general, NOx are composed of nitrogen oxide (NO) and nitrogen dioxide ($NO_2$) [20,21].

All NOx gas hazards in underground mining operations can be grouped into those that appear naturally or those that appear due to technological processes. The natural sources of NOx in an underground mine are the emission of gas from the rock mass or the oxidation of nitrogen from the atmosphere. However, it should be noted that the largest volumes of NOx are generated in processes related to the technological cycle of the mine: welding work, blasting work, and, above all, diesel-powered machinery [2]. The primary source of NOx in the mine atmosphere is technological processes, specifically the operation of diesel machinery [22,23]. One of the main sources of harmful compounds that are released into the mine atmosphere is diesel-powered machinery. Diesel engines generate many chemical compounds in liquid, solid, and, most importantly, gaseous states. The most important of these are sulphur dioxide ($SO_2$), carbon monoxide (CO), carbon dioxide ($CO_2$), hydrocarbon compounds ($CH_x$), nitrogen oxide (NO), nitrogen dioxide ($NO_2$), and solid particles [24–29]. According to Stavert and Lehnert [30] and Kampa [31], NOx is a harmful air pollutant that can have significant impacts on both the environment and human health. Both monoxide NO and dioxide $NO_2$ are odourless gases. Nitrogen monoxide is a colourless gas, while nitrogen dioxide at a certain concentration can take on a brown colour [32,33]. In the exhaust of a diesel engine, the share of nitrogen oxides is about 90% NO and about 10% $NO_2$ [34]. NOx can be a danger to human health, particularly for people with respiratory problems or heart disease. Exposure to high levels of NOx can cause irritation of the eyes and throat, coughing, shortness of breath, and reduced lung function. Long-term exposure to NOx can increase the risk of respiratory infections and chronic lung diseases [35–38]. The more toxic gas is nitrogen dioxide [39], which at 1.5 ppm already causes respiratory problems, while at 5 ppm it leads to a drop in blood pressure. When the $NO_2$ concentration reaches about 200 ppm, it can result in human death [40]. Due to the negative influence of NOx on humans, it is important to monitor the concentrations of nitrogen oxides in underground mines. However, it is even more important to predict the NOx emissions from LHD vehicles and heavy transport trucks, depending on individual working modes. In the case of accurate NOx emissions prediction tool development (a soft sensor), the overall performance of the ventilation system can be optimized and the working atmosphere improved in the underground mine.

Due to the characteristics of NOx and its negative effects on human health, a lot of research is being conducted to improve occupational safety by reducing emissions. Currently, many researchers are working to develop an innovative method to control and predict dangerous gases from diesel engine emissions in underground mines [41,42].

To predict the concentration of dangerous gases in underground mines, air monitoring systems can be installed to continuously monitor the concentrations of various gases in the mine atmosphere. Real-time monitoring of gas concentrations can help to identify potential hazards and enable mine operators to take appropriate measures to control the release of dangerous gases [43–45]. In addition, mathematical models can be developed to predict the concentration of dangerous gases in the mine atmosphere. These models take into account various factors such as ventilation rates, engine emissions, and the physical characteristics of the mine and can help mine operators anticipate dangerous levels of gases and take appropriate measures to mitigate risks [46].

The operation of LHD vehicles is characterized by reverse motion with frequent changes from acceleration to deceleration and repeating cycles, as well as quick transitions from one level of engine load to another [47]. Although the powertrain of these vehicles usually contains a hydraulic torque converter, which reduces torque peaks [48] and smooths torque demand to the engine, there is a big challenge to meet the environmental legislation because of inertia in the flow rate and temperature in exhaust gas recirculation (EGR) systems [49]. To tackle this problem, different models for NOx prediction have been developed and tested both in the lab and real conditions.

A simplified physics-based model of the engine is proposed in [50] to predict NOx emissions by narrow-range inputs. However, fuel combustion in diesel engines is a significantly nonlinear process. Physics-based models cannot account for all influencing parameters due to certain assumptions and simplifications. Therefore, data-driven approaches are also widely used in this domain. The Hammerstein–Wiener model is applied in [51] but for a small region of operation parameters. In work [52], NOx emissions from a diesel engine are modelled with a nonlinear autoregressive with exogenous input (NARX) model. Experimental results show that NOx emissions can be estimated with a reduced set of regressors in order to be more stable and robust.

In [53], the authors proposed a combined grey-box modelling approach with numerical identification of static maps, while the main factors are accounted for by physical assumptions. This model showed a wide range of validity and high accuracy, but the fitting performance in highly dynamic conditions is insufficient.

To capture memory effects, Volterra polynomials were employed in [54] for identification of nonlinear models of diesel engine emissions. An increasing number of inputs and the degree of polynomials increases the set of estimated parameters and makes this approach difficult for practical application. In work [55], the authors give a model for NOx and soot emissions in the form of local linear regression models where the parameters are represented in tables. Then, using the $\beta$-spline function, they find the parameters of a globally optimal model by solving a linear least-squares problem. However, this work is evaluated only for steady-state engine operations.

The authors of work [56] estimated NOx emissions of a heavy-duty diesel engine with engine speed and pressure measurements. Principal component analysis (PCA) and L2 regularization techniques are used to derive a simple and reliable estimator. The developed estimator shows sufficient performance in steady-state regimes but improvements are required for transient cycles of engine loading.

An ANN is employed in [57] to estimate emissions of $CO_2$, NOx, and PM of a Common-Rail Diesel Injection (CRDI) engine. It was shown that increasing the number of hidden layers and neurons causes over-fitting and decreases the generalization of the model.

In the work [58], to solve the engine optimization problem, a multi-layer perception (MLP) neural network followed by multi-objective optimization including a non-dominated sorting genetic algorithm II (NSGA-II) and strength Pareto evolutionary algorithm (SPEA2) were used. This study allowed the authors to decide which algorithm is preferable for optimizing engine emissions and fuel consumption. As an alternative to complicated physics-based models, a multidimensional data-driven approach is proposed in [59] to estimate NOx emissions. Using Deep Neural Networks (DNNs), separate models were developed: engine-out NOx and tailpipe NOx emissions. Two datasets were used from the onboard diagnostic system, namely, an engine dynamometer and a chassis dynamometer. Both the cold/hot Federal Test Procedure (FTP) and the Ramped Mode Cycle (RMC) were applied. The authors proved that high precision of the DNN models ($R^2$ = 0.92–0.95 up to 0.99) can be achieved by utilizing minimal engine and exhaust gas after-treatment parameters.

Another factor affecting diesel engine emissions in articulated heavy-duty underground loaders is the depth of the mine. In [60], engine emissions were determined by a portable gas analyser at various depths from the surface (up to 7000 feet below sea level). Based on the measurement results, the authors concluded that carbon monoxide (CO) and diesel particulate matter (DPM) emissions decrease with depth because of the higher air density and air/fuel ratio for the same parameter set in the vehicle Electronic Control Unit (ECU). Instead, NOx emissions increase with depth. The authors related this to the effect of pressure on in-cylinder NO formation. The influence of ambient air temperature and humidity on NOx emissions is investigated in [61], which noted that an increase in intake air humidity (in the range of 31–80%) causes a 3–14% reduction in the NOx emissions at a constant temperature of 26 °C. The influence of intake air temperature on engine torque and emissions is analysed in [62]. They obtained accurate regression models (RMSE 72.38 and accuracy 99.2%) and discovered that the ambient temperature in the range 5–30 °C has a great influence on both the torque and the prediction of NOx. Nevertheless, since the temperature and humidity at a certain depth and geological conditions of underground mines are approximately constant, these factors can be neglected in the prediction model.

## 3. Measurements

NOx emissions measurements were carried out on a KGHM ZANAM vehicle—more precisely, the LHD LKP-1701 operated in the underground copper ore mine of KGHM Polska Miedź (Poland). This vehicle is depicted in Figure 1, and its general technical specifications are given in Table 1.


**Figure 1.** LKP-1701: the LHD vehicle (KGHM ZANAM) [63].

**Table 1.** Technical specification of LKP-1701 [63].

| Parameter | Value | Units |
|---|---|---|
| Length | 11,500 | mm |
| Width | 3380 | mm |
| Height | 2350 | mm |
| Gross weight | 48,600 | kg |
| Bucket capacity | 8.6 | $m^3$ |
| Lifting capacity | 172 | kN |
| Engine power | 390 | kW |
| Driving speed: | | |
| 1st gear | 5.0 | km/h |
| 2nd gear | 9.0 | km/h |
| 3rd gear | 15.0 | km/h |
| 4th gear | 20.0 | km/h |

The equipment is specifically designed to operate in the confined spaces of low tunnels and is equipped with a DEUTZ TCD 12.0 V6, which is a turbocharged diesel engine and SCR system, as shown in Figure 2. The relationship between diesel engine power and torque can be found in Figure 3, while a comprehensive list of engine parameters is provided in Table 2. It is important to note that the parameters listed are taken directly from the manuals provided by the diesel engine manufacturer, and the best point consumption refers to diesel fuel with a density of 0.835 kg/$dm^3$ at 15 °C.

**Table 2.** The power and torque functions of diesel engine DEUTZ TCD 12.0 V6 [64].

| Parameter | Value | Units |
|---|---|---|
| Power output as per ISO 14396 | 390 | kW |
| at speed | 2100 | rpm |
| Max. torque | 2130 | Nm |
| at speed | 1400 | rpm |
| Min. idling speed | 600 | rpm |
| Specific fuel consumption | 194 | g/kWh |

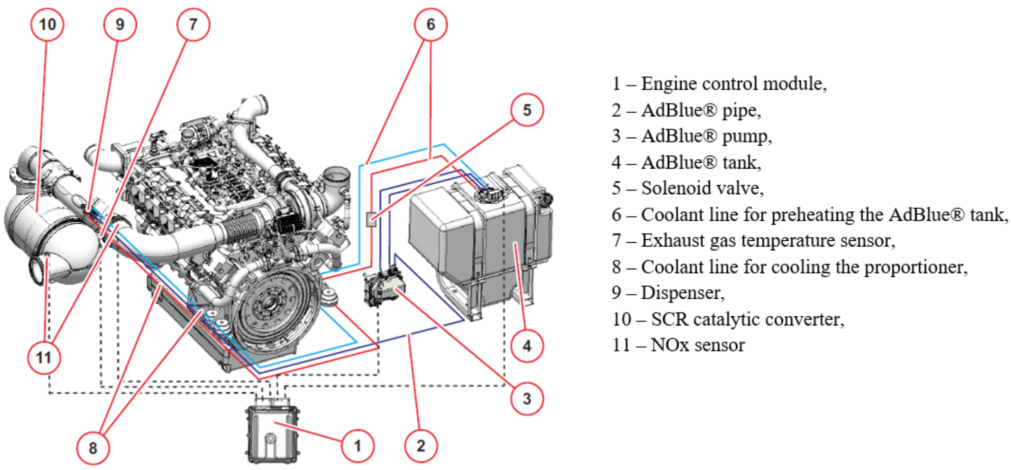


**Figure 2.** The DEUTZ TCD 12.0 V6 diesel engine with its SCR system [64].

Diesel engines are usually operated with an overstoichiometric air-to-fuel ratio to provide the full combustion of soot and to restrict exhausting unburnt fuel. Excess air leads to high NOx emissions. This engine produces 390 kW of power and contains a BlueTec system for exhaust gas after-treatment. This process of NOx emissions reduction is carried out by selective catalytic reduction (SCR) with an ammonia slip catalytic converter and diesel oxidation catalytic converter (DOC). SCR uses Diesel Exhaust Fluid (DEF), or

AUS 32 (Aqueous Urea Solution 32%) by ISO 22241. DEF from a special tank is injected into the exhaust pipeline to decompose it to ammonia by the exhaust heat. Inside the SCR catalyst, the ammonia reduces NOx into non-polluting water and nitrogen, which is then released into the atmosphere. The exhaust gas after-treatment unit reads signals from the sensors and transmits them via CAN bus to the engine management control unit: temperature upstream of the SCR catalytic converter; temperature downstream of the SCR; NOx downstream of the SCR; pressure (fluid level) and temperature in the AdBlue/DEF tank; and intake air humidity and temperature.

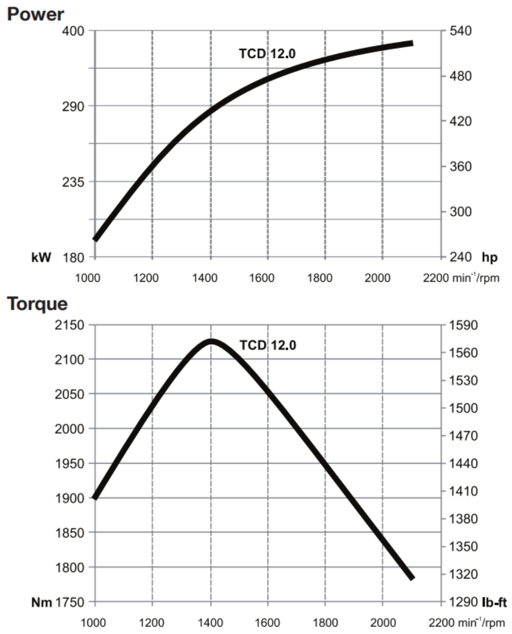


**Figure 3.** The power and torque functions of diesel engine DEUTZ TCD 12.0 V6 [64].

Table 3 presents the standard parameters of the NOx sensor. However, under current regulations, NOx mass measurements must have a minimum accuracy of ±20% or ±0.1 g/bhp-h [65], which most NOx sensors cannot achieve under transient load conditions. The causes of this include cross-sensitivity to ammonia ($NH_3$), exhaust gas flow rate, mass air flow (MAF), or sensor position. Additionally, many sensors have noise levels as low as 10 ppm due to residual amounts of NOx in the exhaust system even when the NOx concentration is zero [66].

**Table 3.** Parameters of the NOx sensor.

| Parameter | Value | Units |
|---|---|---|
| Measuring range (NOx) | 0–1500 | ppm |
| Accuracy | ±10(20) | % |
| Operating temperature | −40...105 | °C |
| Exhaust temperature | <800 | °C |

Development and validation of a vibration-based virtual sensor are conducted in [67] for real-time monitoring of NOx emissions from a diesel engine. The virtual NOx sensor is validated on a single-cylinder diesel engine bench. The prediction error was less than ±10% for the steady-state mode and below ±20% for transient conditions. The NOx prediction model is based on principal component regression (PCR). Unfortunately, in this approach, an additional sensor is required to reconstruct the in-cylinder pressure from the vibration signal. The application of this virtual NOx sensor for multi-cylinder engines probably requires more sensors or advanced signal processing techniques.

The onboard monitoring system obtains parameters of LHD vehicle operation and the diesel engine via CAN bus, stores them locally, and uploads data to the enterprise server via a wireless connection once per working shift (about 6 h). Almost all monitored parameters are sampled with a time interval of 1 s and are given in Table 4.

**Table 4.** Parameters of LHD operation taken from the onboard monitoring system for NOx emission analysis.

| No. | Parameter | Description | Units |
|---|---|---|---|
| | **ENGNOX** | NOx Emissions | ppm |
| 1 | **ENGCOOLT** | Coolant temperature | °C |
| 2 | **ENGOILT** | Oil Temperature | kPa |
| 3 | **ENGRPM** | Engine rotations | rpm |
| 4 | **ENGTPS** | Engine acceleration | % |
| 5 | **FUELUS** | Fuel consumption | L/h |
| 6 | **GROILP** | Gear oil pressure | kPa |
| 7 | **GROILT** | Gear oil temperature | C |
| 8 | **HYDOILP** | Hydraulic oil pressure | MPa |
| 9 | **INTAKEP** | Intake air pressure | kPa |
| 10 | **INTAKET** | Intake air temperature | °C |
| 11 | **SPEED** | Vehicle speed | km/h |
| 12 | SELGEAR | Selected gear | −4…0…4 |

## 4. Methodology of NOx Prediction

*Multi-Layer Perceptron (MLP) Network*

One of the most popular ANNs frequently used in engineering, medicine, and mathematical modelling applications is a Multi-Layer Perceptron (MLP) network [68,69]. A Multi-Layer Perceptron (MLP) network is a type of neural network that consists of multiple layers of interconnected nodes (or neurons) arranged in a feedforward manner. It is a supervised learning algorithm used for classification and regression tasks. The structure of an MLP neural network is composed of input units, hidden units, and output units (see Figure 4). Inputs are multiplied by weights and added to bias conditions to form a weighted sum. The activation level of each unit is calculated by applying a transfer function to the weighted sum and bias condition. The MLP is deployed in a layered feed-forward topology in which information flows in only one direction from the input layer through the hidden layers to the output layer. This structure is commonly referred to as a Feed-Forward Neural Network. Each layer has several processing units and is fully interconnected with weighted connections to units in the subsequent layer. The MLP transforms $n$ inputs to $l$ outputs through some nonlinear functions [70–72].

In our case, multiple inputs (LHD working parameters) and only one output (NOx value) are considered.

$$\begin{aligned} x_t &= A_{t-1}x_{t-1} + q_t \\ y_t &= H_t x_t + r_t \end{aligned} \tag{1}$$

Based on a dataset with input parameters obtained from the LHD monitoring system, this ANN was trained. Then, tests were conducted to validate the accuracy of the NOx prediction.

The ANN created for solving the NOx emission prediction problem consists of 1 input layer, 1 hidden layer, and 1 output layer. For inputs, 11 parameters are used, and the output is only 1 − NOx emission level. In the hidden layer, 20 neurons are used. Input data are normalized to the range $[-1, 1]$, and the transfer functions used are hyperbolic tangent sigmoid for the hidden layer and linear for the output layer. As a loss function, MSE was chosen. Data are split using random sampling into 3 datasets—training data (70%), validation data (15%), and test data (15%).

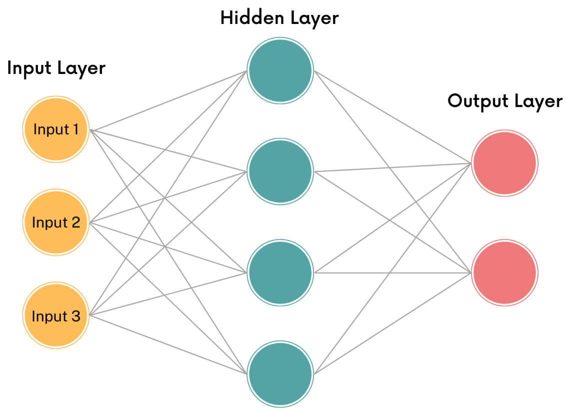


**Figure 4.** The structure of a Multi-Layer Perceptron (MLP) network.

## 5. Data Analysis

### *5.1. Preliminary Analysis and Input Variable Selection*

The time series of the LHD operation parameters and the corresponding NOx emission amounts are represented in Figures 5 and 6. Both graphs have grid lines of time equal to 60 s. To make the graphs more suitable for comparison, time series are re-sampled by a linear moving average filter (5 points or 5 s). In this way, the sharp changes of operational parameters are equalized to the NOx sensor output and the intake pressure signal INTAKEP (kPa), which is originally sampled with a 5 s period by the onboard monitoring system.

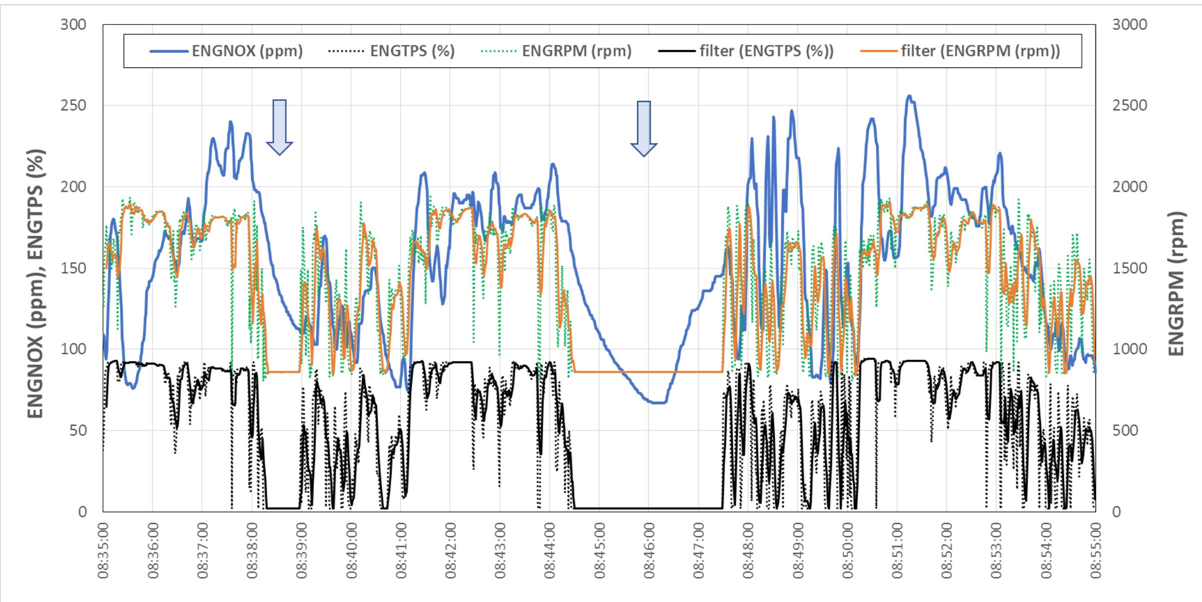


**Figure 5.** The time series of recorded signals: NOx emission ENGNOX (ppm); engine rotations ENGRPM (rpm); and engine acceleration ENGTPS (%).

Looking at the graphs in Figure 5, we can conclude that engine rotations expectedly follow the engine acceleration (operator's pedal), and both signals are well-correlated with NOx sensor output and a certain delay in its reaction, i.e., such a natural logical sequence of signals exists: "acceleration–rotations–emission".

During every period of idle engine rotations (pointed out by the arrows in the graph) at about 855 rpm without acceleration (stable value of 2%), the NOx emission signal gradually falls to a minimum value (about 68 ppm) and then rises. The maximum value of the NOx signal observed in the given whole dataset is equal to 1650 ppm. Hence, the NOx sensor output is non-linearly dependent on the idle mode duration. This effect is difficult to account for in the ANN-based model. These periods of time can be excluded from model training by the logical condition: (ENGTPS = 2% and ENGRPM < 860 rpm). By comparison, the logical condition (ENGTPS = 2% and ENGRPM = 0 rpm) corresponds to a fully stopped engine. In this case, engine acceleration remains non-zero (2%), too, which is probably related to signal bias in the monitoring system.

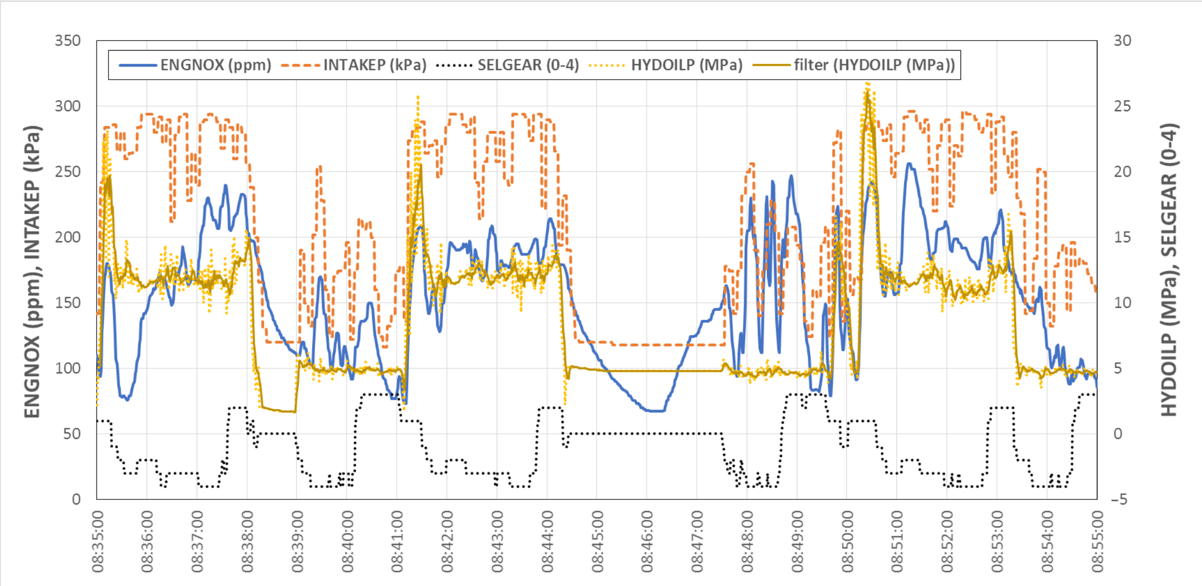


**Figure 6.** The time series of recorded signals: NOx emission ENGNOX (ppm); intake air pressure INTAKEP (kPa); selected gear (−4. . .0. . .4); and hydraulic oil pressure HYDOILP (MPa).

The graphs in Figure 6 have the same time axis as in Figure 5 but show parallel to the NOx sensor output other signals potentially suitable for ANN-based model training.

The value of the selected gear SELGEAR (−4. . .0. . .4) reflects the operator's control of the engine load and its rotations (output torque), including reverse motion (negative values). As previously, the same periods of idle rotation of the engine are presented in this graph when SELGEAR = 0. Therefore, this logical condition can be added to exclude data points in the ANN-based model training of NOx prediction.

Hydraulic oil pressure HYDOILP (MPa) corresponds to the "load–haul–dump" cycles of the LHD vehicle and reaches maximum values at the beginning of every cycle when the operator fills the bucket by digging into the hill of blasted bulk rock. These peaks in hydraulic pressure are well-correlated with the maximum engine acceleration rate (100%) at a rotation speed of 1700 rpm and the lowest selected gear (1). However, during the transportation period, the NOx emission signal is almost uncorrelated with this parameter, demonstrating more frequent oscillations of small amplitude around a certain value until the moment of unloading.

The intake air pressure signal INTAKEP (kPa) is responsible for the fuel combustion process and is well-correlated with NOx emission. Even having a lower sampling frequency (5 s), this signal can be a good candidate for inclusion into input parameters for ANN-based model training and further NOx prediction.

The correlations of the most-dependable parameters are shown in Figure 7 and are constructed from the data subset without idle modes. The ENGNOX (ppm) non-linear relation with ENGTPS (%) has $R^2$ = 0.2298, and the linear relation with INTAKEP (kPa) has $R^2$ = 0.5278, which are not satisfactory for NOx prediction in practice.

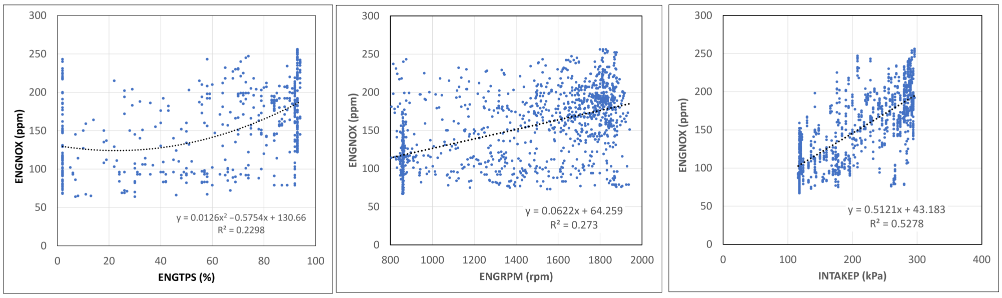


**Figure 7.** The correlation of LHD operational parameters.

Over the selected dataset, the calculated average value of NOx emissions is about 122 ppm over all the working cycles of the LHD. The standard deviation from the average value is 47 ppm. The upper limit is 428 ppm, while the lower values (at the idle engine rotation speed without load) are about 68 ppm. The NOx value for the stopped engine is 56 ppm. This value is more likely to be due to bias of the sensor or a result of the gas action that still remains in the exhaust system. It should be noted that the measuring sensor is installed in the exhaust pipe of the tested machine. The harmful gases that escape into the mine atmosphere from the machine are diluted with air; for example, NO values should not exceed 2.6 ppm in Poland [73].

### 5.2. *MLP Training, Validation, and Testing*

The results of MLP network training, validation, and testing over separate datasets along with the Mean Squared Error (MSE) and the Root Mean Squared Error (RMSE) are represented in Figures 8–11. The correlation of original data with predicted data is also shown in those graphs.

In the following, the results of the proposed methodology are presented for two different cases: (1) modelling in the presence of the outliers and (2) modelling after removing the outliers. The condition NOx > 3 × STD (standard deviation) was used as a criterion to reject outliers from the dataset. In this research, as was noted before, 70% of the data were used as the training dataset, 15% for validation, and the remaining 15% for testing.

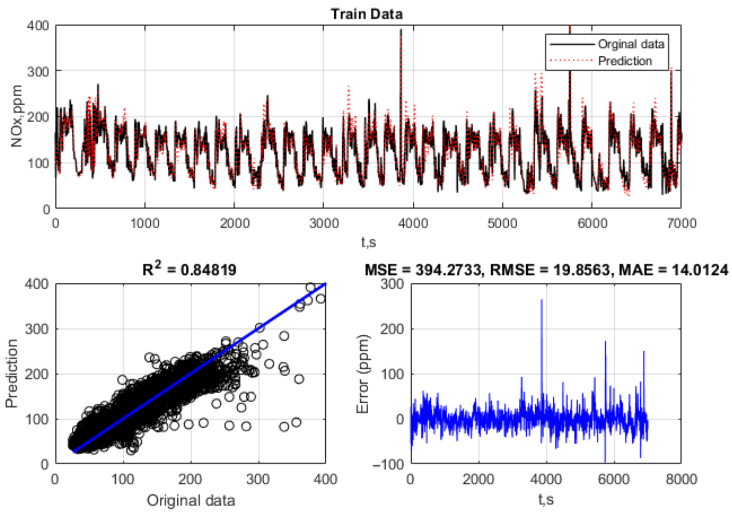


**Figure 8.** Training data.

#### 5.2.1. Results with Outliers

Figures 8–11 show the results for training data, validation, testing, and all data with outliers. In Figure 8, results of the proposed methodology for the training dataset in the presence of outliers are presented. As seen in the training data panel of this figure, the proposed approach could predict the data correctly. However, we can see some areas around the 3800 and 5200 samples that have been overestimated. Furthermore, the $R^2$ and error for the training data are presented.

In Figure 9, the results of the proposed methodology for the validation data in the presence of outliers are presented. As seen in the validation data panel of this figure, the proposed approach could predict the data with acceptable results. However, as in the previous one, we can see some areas around the 800 and 1200 samples that have been overestimated. Furthermore, the $R^2$ and error values are presented for the validation data.

The results of the proposed approach are shown in Figure 10. As seen in the test data panel of this figure, the results are acceptable. However, we can see some areas around samples 800 and 1200 that have been overestimated. Furthermore, the $R^2$ and error values are presented for the test data.

In the end, all data results are presented in Figure 11. As expected, based on the previous plots in this figure, we can see some areas around the 5800 and 7800 samples that have been overestimated.

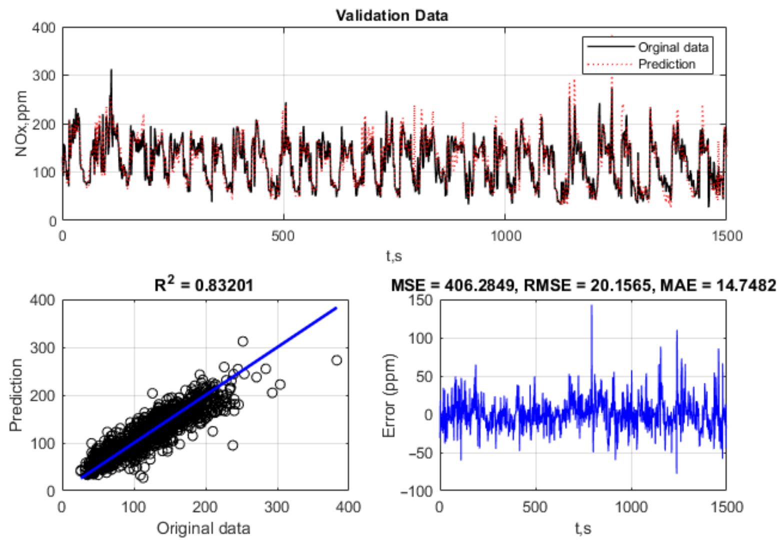


**Figure 9.** Validation data.

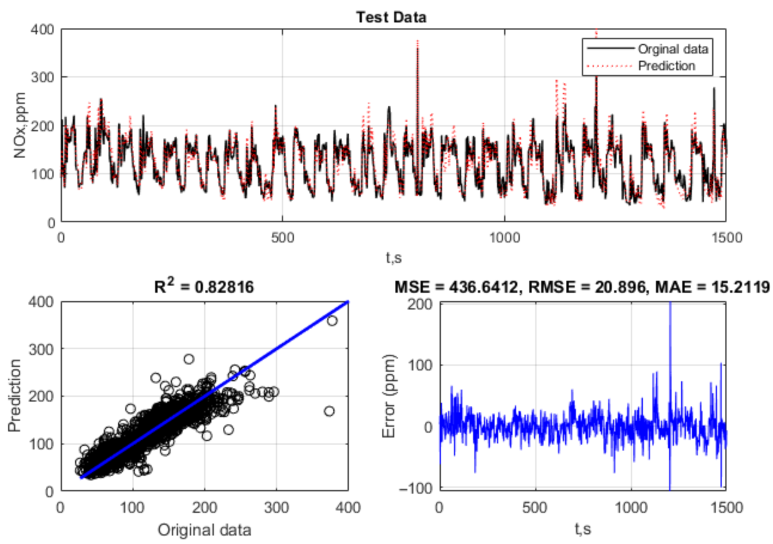


**Figure 10.** Test data.

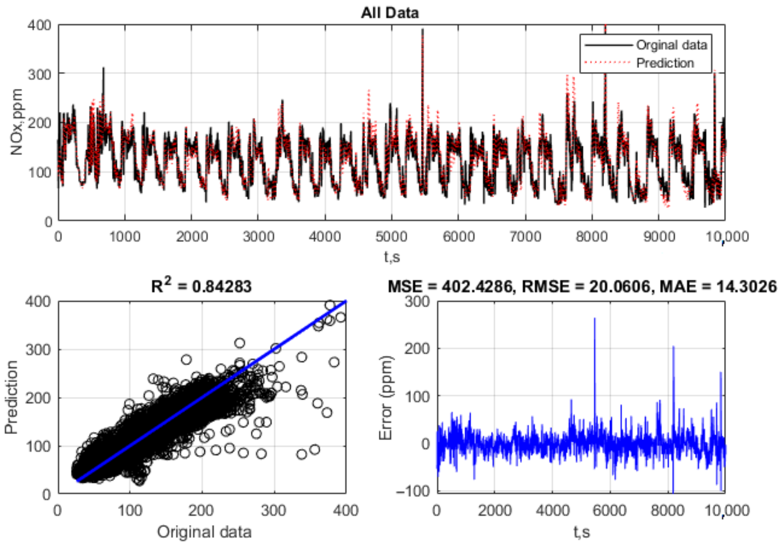


**Figure 11.** All data with outliers.

#### 5.2.2. Results without Outliers

Figures 12–15 show the results for training data, validation, testing, and all data after outlier removal. In Figure 12, results are presented of the proposed methodology for the training dataset with outliers removed. As can be seen in the training data panel of Figure 12, the proposed approach could predict data precisely. Also, in some areas, we can see some overestimated data; however, compared with the previous case, there are fewer errors.

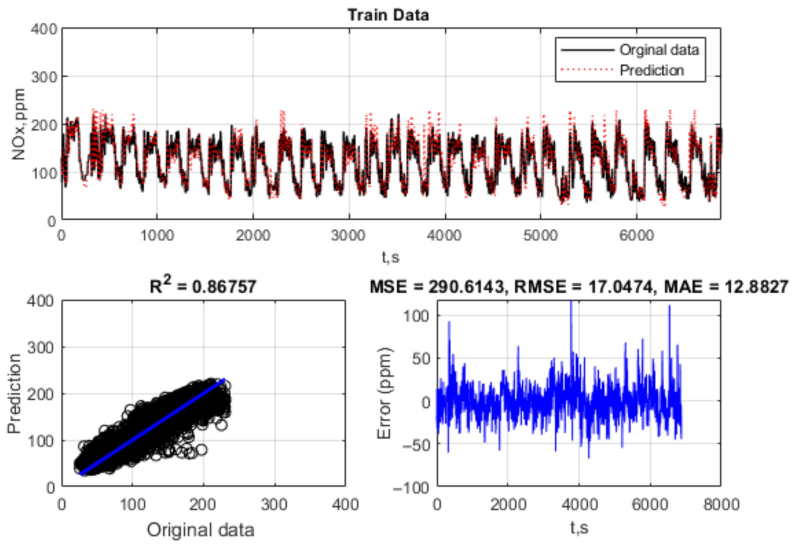


**Figure 12.** Training data.

The results of the proposed approach for the validation and test data are presented in Figure 13 and Figure 14, respectively. Finally, the result for all data is presented in Figure 15. Also, as we expected, these results had fewer errors than in the previous case with outliers.

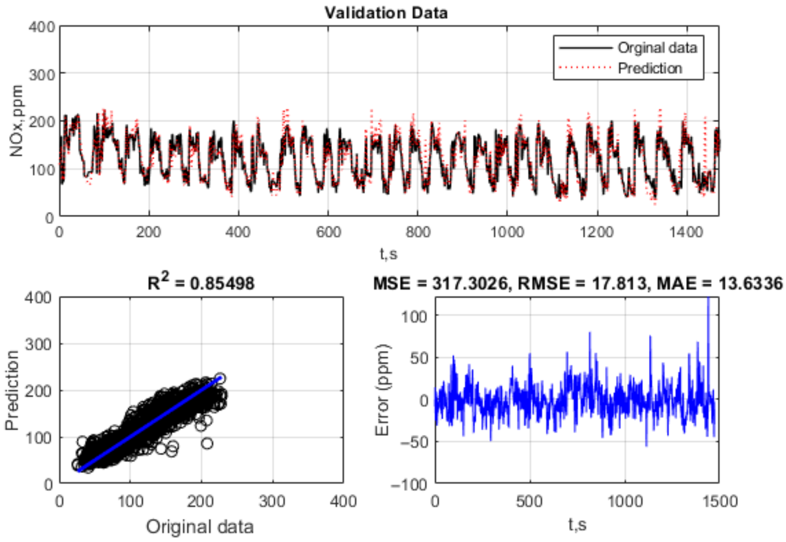


**Figure 13.** Validation data.

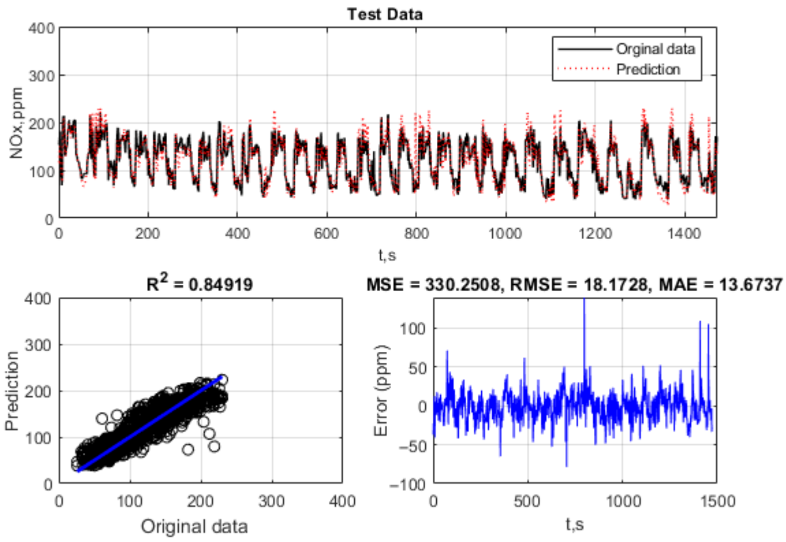


**Figure 14.** Test data.

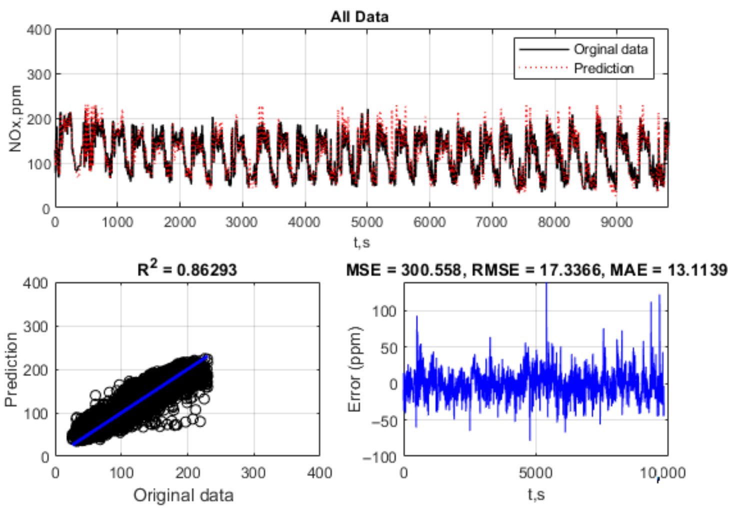


**Figure 15.** All data.

## 6. Discussion

The accuracies of the NOx emissions prediction achieved in the training, validation, and testing datasets are given in Table 5. To check the robustness of the developed ANN-based model, different statistical metrics are used.

**Table 5.** Errors of NOx emission prediction for datasets.

| Errors | Training | Validation | Testing | All Data | Units |
|---|---|---|---|---|---|
| Mean Average Error (MAE) | 12.8827 | 13.6737 | 13.6737 | 13.1139 | ppm |
| Mean Squared Error (MSE) | 290.6143 | 317.3026 | 330.2508 | 300.558 | — |
| Root Mean Squared Error (RMSE) | 17.0474 | 17.813 | 18.1728 | 17.3366 | ppm |
| Coefficient of determination ($R^2$) | 0.86757 | 0.85498 | 0.84919 | 0.86293 | — |

The cumulative error of the NOx prediction over time is shown in Figure 16 for all data. The coefficient of determination seems high—up to 0.86757—and the total deviation of NOx emissions is moderate during half of the working shift (about 3 h).

Using the ANN-based MLP model for the prediction of NOx emissions allows the estimation of the environmental impacts of LHD vehicles working in the underground mine and equipped with the monitoring system. Since not every LHD has a NOx sensor, the results obtained can easily be implemented on a large number of working machines.

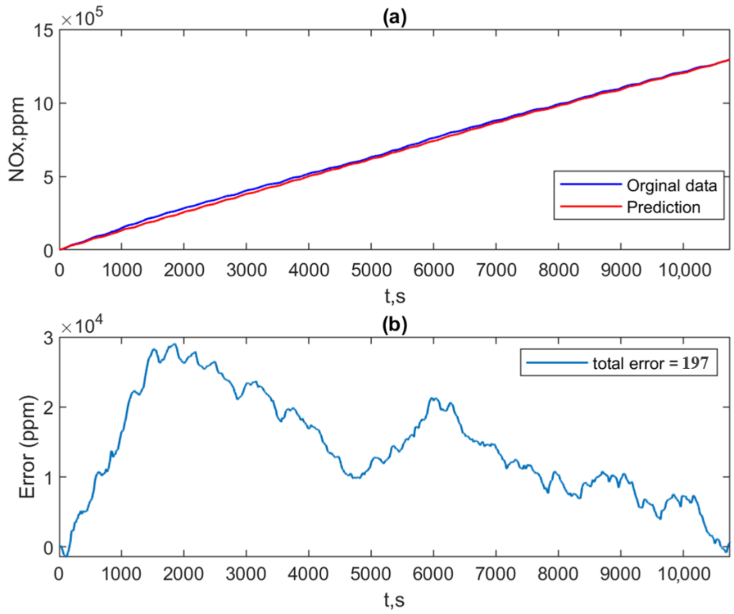


**Figure 16.** Cumulative NOx emissions: original measured data and predicted (**a**); error of MLP prediction (**b**).

The main problem in NOx prediction is to account for the transient modes of LHD bucket filling, acceleration, and deceleration when the engine is subjected to maximum loading and fuel combustion. However, following the analysed dataset, which represents many working cycles, the duration of several outliers in NOx emission is very short (several seconds) compared to the entire time; therefore, the amount of NOx is less than 1%. Therefore, before ANN training, those samples can be rejected, which greatly improves prediction accuracy (up to 85%). The criterion for outlier rejection from the dataset can be a condition of NOx > 3 × STD (standard deviation), i.e., beyond the Gaussian distribution range.

For longer distances of delivery, i.e., fewer LHD cycles per working shift, the accuracy of predictions is expected to be higher due to more-stable modes of diesel engine loading with fewer transient periods. Pieces of blasted material with bigger sizes create a greater load on the engine when the LHD bucket penetrates the hill; hence, heterogeneous material will reduce the accuracy of NOx prediction.

Future research is directed toward improving the prediction of NOx emissions in transient modes of operation of LHD vehicles (e.g., excavation of bulk material and reverse motion). This ANN-based "soft-sensor" can be utilized in ventilation power demand estimation in certain geological conditions of underground mining, which accounts for material granulation after blasting, road inclination, and distance of delivery to dumping points. In addition, trend analysis in NOx emission of certain LHD vehicles can be used for the assessment of individual operator driving qualifications. Further, trends of NOx emissions in certain LHD vehicles over all operators can demonstrate malfunctions in fuel injection or after-treatment systems as well as supplied fuel quality.

## 7. Conclusions

Based on the real data of LHD vehicle operations and conducted research for NOx emission prediction, the following conclusions can be derived:

1. **The MLP models analysed in this article were developed based on the selected input parameters.** The decision was made to include 11 parameters that were measured using the SYNAPSA system. The selection of parameters was based on their impact on the emission of NOx.
2. **ANN-based models can be an efficient tool for NOx emission prediction of heavy-duty diesel engines installed in the powerful underground LHD vehicles working in transient modes of loading and speeds.** The environmental conditions in which mining machinery operates are hard. The solution presented in the article aims to improve the safety of underground crews. Since most industrial vehicles with diesel engines are not equipped with sensors that measure the concentrations of harmful gases, the proposed solution for modelling NOx concentrations will provide a better understanding of the atmosphere of the working environment. The coefficient of determination is 0.86293, which the authors consider a satisfactory result for such complex industrial data. The ability to predict average exhaust emissions will allow for controlling gas hazards in underground mine work.
3. **The created ANN-based model should be tested and adapted over bigger datasets for different geological conditions (blasted material, road inclination, surface watering, and transportation distances) and operator experience with different driving manners.** In further research, the model proposed in the article should be expanded to include more parameters. It is also necessary to test the operation of machines under different geological and hydrogeological conditions. This activity will make it possible to create appropriate models for predicting NOx from mining machines operating under specific geological and mining conditions.
4. **Data prediction values of NOx emission concentrations in mine work can be the basis for manoeuvring the ventilation airflow.** By incorporating this information into the ventilation system power demand and capacity planning, the ventilation system can be optimized to ensure safe working conditions for the miners. The statistical method proposed in the article provides a way to estimate NOx concentrations that will be present in the mine atmosphere based on various factors such as production plans, a fleet of vehicles, and transportation routes. Knowing this information, ventilation services can adjust the ventilation system accordingly, which can help reduce the risk of health problems caused by high concentrations of NOx in the workplace. Increasing the air volume flow is just one example of how the ventilation system can be adjusted to manage NOx concentrations, and there may be other strategies that can be used as well.

The aim of this study was to develop an ANN-based method (estimator or "soft sensor") applicable in practice for NOx emissions prediction based on LHD monitoring parameters. This aim was achieved, and the developed procedure is intended for implementation as an additional function (module) in the SYNAPSA system. Following studies will be devoted to the investigation of other underground vehicles (hauling trucks) equipped with different diesel engines and working in other mines and geological conditions.

**Author Contributions:** Conceptualization, R.Z. and A.B.; methodology, R.Z.; software, F.M. and M.K.; validation, P.K., P.Ś. and R.Z.; formal analysis, P.Ś. and J.W.; investigation, A.B. and P.Ś.; resources, R.Z.; data curation, F.M., M.K., P.K. and J.W.; writing—original draft preparation, A.B., F.M. and P.K.; writing—review and editing, A.B. and P.K.; visualization, F.M., J.W. and M.K.; supervision, R.Z. and P.Ś.; project administration, A.B.; funding acquisition, R.Z. All authors have read and agreed to the published version of the manuscript.

**Funding:** This work is supported by the European Institute of Innovation and Technology (EIT), a body of the European Union, under Horizon Europe, the EU Framework Programme for Research and Innovation: EIT RawMaterials GmbH under Framework Partnership Agreement No. 21119 (VOT3D—Ventilation Optimizing Technology based on 3D-scanning).

**Institutional Review Board Statement:** Not applicable.

**Informed Consent Statement:** Not applicable.

**Data Availability Statement:** Data is unavailable due to privacy restrictions.

**Conflicts of Interest:** The authors declare no conflict of interest. The authors declare that they have no known competing financial interests or personal relationships that could have appeared to influence the work reported in this paper.

## Abbreviations

The following abbreviations are used in this manuscript:

| | |
|---|---|
| LHD | Load–haul–dumping Vehicle |
| ANN | Artificial Neural Network |
| MLP | Multi-Layer Perceptron |
| NOx | Nitrogen Oxides |
| SCR | Selective Catalytic Reduction |
| DOC | Diesel Oxidation Catalyst |
| ECU | Electronic Control Unit |
| DNN | Deep Neural Network |
| FTP | Federal Test Procedure |
| RMC | Ramped Mode Cycle |
| DPM | Diesel Particular Matter |
| DEF | Diesel Exhaust Fluid |
| MAF | Mass Airflow |
| PCR | Particular Component Regression |
| MSE | Mean Squared Error |
| RMSE | Root Mean Squared Error |

## References

1. Kurnia, J.C.; Sasmito, A.P.; Wong, W.Y.; Mujumdar, A.S. Prediction and innovative control strategies for oxygen and hazardous gases from diesel emission in underground mines. *Sci. Total. Environ.* **2014**, *481*, 317–334. [CrossRef]
2. Banasiewicz, A.; Janicka, A.; Michalak, A.; Włostowski, R. Photocatalysis as a method for reduction of ambient NOx in deep underground mines. *Measurement* **2022**, *200*, 111453. [CrossRef]
3. Dong, L.; Tong, X.; Li, X.; Zhou, J.; Wang, S.; Liu, B. Some developments and new insights of environmental problems and deep mining strategy for cleaner production in mines. *J. Clean. Prod.* **2019**, *210*, 1562–1578. [CrossRef]
4. Strumiński, A.; Madeja-Strumińska, B. Mine ventilation practice in Polish copper mines. In *Mining in the New Millennium Challenges and Opportunities*; CRC Press: London, UK, 2020; pp. 173–179.
5. Hebda-Sobkowicz, J.; Gola, S.; Zimroz, R.; Wyłomańska, A. Identification and statistical analysis of impulse-like patterns of carbon monoxide variation in deep underground mines associated with the blasting procedure. *Sensors* **2019**, *19*, 2757. [CrossRef] [PubMed]
6. Tutak, M.; Brodny, J.; Szurgacz, D.; Sobik, L.; Zhironkin, S. The Impact of the Ventilation System on the Methane Release Hazard and Spontaneous Combustion of Coal in the Area of Exploitation—A Case Study. *Energies* **2020**, *13*, 4891. [CrossRef]
7. Szlęzak, N.; Obracaj, D.; Borowski, M. Methods for controlling temperature hazard in Polish coal mines. *Arch. Min. Sci.* **2008**, *53*, 497–510.
8. Shote, A.S.; Betiku, E.; Asere, A.A. Characteristics of CO and NOx emissions from combustion of transmethylated palm kernel oil-based biodiesel blends in a compression ignition engine. *J. King Saud Univ.-Eng. Sci.* **2019**, *31*, 178–183. [CrossRef]

9. Borowski, M.; Życzkowski, P.; Cheng, J.; Łuczak, R.; Zwolińska, K. The Combustion of Methane from Hard Coal Seams in Gas Engines as a Technology Leading to Reducing Greenhouse Gas Emissions—Electricity Prediction Using ANN. *Energies* **2020**, *13*, 4429. [CrossRef]
10. Ghalandari, M.; Fard, H.F.; Birjandi, A.K.; Mahariq, I. Energy-related carbon dioxide emission forecasting of four European countries by employing data-driven methods. *J. Therm. Anal. Calorim.* **2020**, *144*, 1999–2008. [CrossRef]
11. Zhou, L.; Cao, Q.; Yu, K.; Wang, L.; Wang, H. Research on Occupational Safety, Health Management and Risk Control Technology in Coal Mines. *Int. J. Environ. Res. Public Health* **2018**, *15*, 868. [CrossRef]
12. Hebda-Sobkowicz, J.; Gola, S.; Zimroz, R.; Wyłomańska, A. Pattern of H2S concentration in a deep copper mine and its correlation with ventilation schedule. *Measurement* **2019**, *140*, 373–381. [CrossRef]
13. Zhao, W.; Cheng, Y.; Pan, Z.; Wang, K.; Liu, S. Gas diffusion in coal particles: A review of mathematical models and their applications. *Fuel* **2019**, *252*, 77–100. [CrossRef]
14. Trzop, K.; Palka, D.; Szurgacz, D.; Sobik, L. Preventive measures to minimize natural hazards in the Polish underground mining industry. *IOP Conf. Ser. Earth Environ. Sci.* **2021**, *684*, 012009. [CrossRef]
15. Bugarski, A.D.; Cauda, E.G.; Janisko, S.J.; Mischler, S.E.; Noll, J.D. *Diesel Aerosols and Gases in Underground Mines; Guide to Exposure Assessment and Control*. Report of Investigations 9687, Department of Health and Human Services Centers (DHHS) for Disease Control and Prevention, National Institute for Occupational Safety and Health, Office of Mine Safety and Health Research; DHHS Publications: Pittsburgh, PA, USA, 2011.
16. COMMISSION DIRECTIVE (EU) 2017/164 of 31 January 2017 Establishing a Fourth List of Indicative Occupational Exposure Limit Values Pursuant to Council Directive 98/24/EC, and Amending Commission Directives 91/322/EEC, 2000/39/EC and 2009/161/EU, Official Journal of the European Union, 1.2.2017. Available online: https://eur-lex.europa.eu/legal-content/EN/TXT/PDF/?uri=CELEX:32017L0164&from=MT (accessed on 30 July 2023).
17. Szlązak, N.; Obracaj, D.; Swolkień, J. Enhancing safety in the Polish high-methane coal mines: An overview. *Mining Metall. Explor.* **2020**, *37*, 567–579. [CrossRef]
18. Wróblewski, A.; Wodecki, J.; Trybała, P.; Zimroz, R. A Method for Large Underground Structures Geometry Evaluation Based on Multivariate Parameterization and Multidimensional Analysis of Point Cloud Data. *Energies* **2022**, *15*, 6302. [CrossRef]
19. Peng, S.; Huang, Z.; Dong, D. Numerical Simulation Study on Fire Hazard of a Coal Mine Transport Roadway. *Min. Scince* **2022**, *29*. [CrossRef]
20. Lasek, J.A.; Lajnert, R. On the Issues of NOx as Greenhouse Gases: An Ongoing Discussion. . . . *Appl. Sci.* **2022**, *12*, 10429. [CrossRef]
21. Rößler, M.; Velji, A.; Janzer, C.; Koch, T.; Olzmann, M. Formation of Engine Internal $NO_2$: Measures to Control the $NO_2$/NOx Ratio for Enhanced Exhaust after Treatment. *SAE Int. J. Engines* **2017**, *10*, 1880–1893. [CrossRef]
22. Banasiewicz, A. Analysis of historical changes in the limit value of nitrogen oxides concentrations for underground mining. *IOP Conf. Ser. Earth Environ. Sci.* **2021**, *684*, 012018. [CrossRef]
23. Debia, M.; Couture, C.; Njanga, P.E.; Neesham-Grenon, E.; Lachapelle, G.; Coulombe, H.; Hallé, S.; Aubin, S. Diesel engine exhaust exposures in two underground mines. *Int. J. Min. Sci. Technol.* **2017**, *27*, 641–645. [CrossRef]
24. Chang, P.; Xu, G. A review of the health effects and exposure-responsible relationship of diesel particulate matter for underground mines. *Int. J. Min. Sci. Technol.* **2017**, *27*, 831–838. [CrossRef]
25. Chang, P.; Xu, G. Review of Diesel Particulate Matter Control Methods in Underground Mines. In *Proceedings of the 11th International Mine Ventilation Congress*; Springer: Singapore, 2019; pp. 461–470. [CrossRef]
26. Noll, J.; Mischler, S.; Schnakenberg, G.; Bugarski, A.; Mutmansky, J.; Ramani, R. Measuring diesel particulate matter in underground mines using sub micron elemental carbon as a surrogate. In Proceedings of the 11th US north American Mine Ventilation Symposium, University Park, PA, USA, 5–7 June 2006; Taylor & Francis: State College, PA, USA, 2006; Volume 2006, pp. 105–110.
27. Liu, X.; Nie, W.; Hua, Y.; Liu, C.; Guo, L.; Ma, W. Behavior of diesel particulate matter transport from subsidiary transportation vehicle in mine. *Environ. Pollut.* **2021**, *270*, 116264. [CrossRef] [PubMed]
28. Kęska, A.; Janicka, A. Evaluation of toxicity of hydrocarbons emitted by Euro 3 and Euro 6 vehicles at idle conditions by means of equivalent toxicity coefficients. *Int. J. Engine Res.* **2022**. [CrossRef]
29. Kolanek, C.; Reksa, M.; Walkowiak, W.; Janicka, A. The future of alternative fuels for internal combustion engines applications. *J. Pol. CIMAC* **2010**, *5*, 77–83.
30. Stavert, D.; Lehnert, B. Nitric oxide and nitrogen dioxide as inducers of acute pulmonary injury when inhaled at relatively high concentrations for brief periods. *Inhal. Toxicol.* **1990**, *2*, 53–67. [CrossRef]
31. Kampa, M.; Castanas, E. Human health effects of air pollution. *Environ. Pollut.* **2008**, *151*, 362–367. [CrossRef] [PubMed]
32. Abdelsalam, E.M.; Mohamed, Y.; Abdelkhalik, S.; El Nazer, H.A.; Attia, Y.A. Photocatalytic oxidation of nitrogen oxides (NOx) using Ag-and Pt-doped $TiO_2$ nanoparticles under visible light irradiation. *Environ. Sci. Pollut. Res.* **2020**, *27*, 35828–35836. [CrossRef]
33. Chuvashev, A.N.; Chuprakov, A.I. Investigation of environmental indicators of diesel engine when working on methanol. *J. Phys. Conf. Ser.* **2019**, *1399*, 055085. [CrossRef]
34. Galbreath, K.C.; Zygarlicke, C.J.; Tibbetts, J.E.; Schulz, R.L.; Dunham, G.E. Effects of $NO_x$, $\alpha$-$Fe_2O_3$, $\gamma$-$Fe_2O_3$, and HCl on mercury transformations in a 7-kW coal combustion system. *Fuel Process. Technol.* **2005**, *86*, 429–448. [CrossRef]

35. Pfeffer, P.E.; Donaldson, G.C.; Mackay, A.J.; Wedzicha, J.A. Increased Chronic Obstructive Pulmonary Disease Exacerbations of Likely Viral Etiology Follow Elevated Ambient Nitrogen Oxides. *Am. J. Respir. Crit. Care Med.* **2019**, *199*, 581–591. [CrossRef]
36. Manisalidis, I.; Stavropoulou, E.; Stavropoulos, A.; Bezirtzoglou, E. Environmental and Health Impacts of Air Pollution: A Review. *Front. Public Health* **2020**, *8*, 14. [CrossRef] [PubMed]
37. Gaston, B.; Drazen, J.M.; Loscalzo, J.; Stamler, J.S. The biology of nitrogen oxides in the airways. *Am. J. Respir. Crit. Care Med.* **1994**, *149*, 538–551. [CrossRef]
38. Pacher, P.; Beckman, J.S.; Liaudet, L. Nitric Oxide and Peroxynitrite in Health and Disease. *Physiol. Rev.* **2007**, *87*, 315–424. [CrossRef]
39. Hori, M.; Matsunaga, N.; Malte, P.C.; Marinov, N.M. The effect of low-concentration fuels on the conversion of nitric oxide to nitrogen dioxide. *Symp. (Int.) Combust.* **1992**, *24*, 909–916. [CrossRef]
40. Özmen, İ.; Aksoy, E. Respiratory emergencies and management of mining accidents. *Turk. Thorac. J.* **2015**, *16*, S18. [CrossRef]
41. Shriwas, M.; Pritchard, C. Ventilation Monitoring and Control in Mines. *Mining Metall. Explor.* **2020**, *37*, 1015–1021. [CrossRef]
42. Banasiewicz, A.; Sliwinski, P.; Krot, P.; Wodecki, J.; Zimroz, R. Prediction of NOx Emission Based on Data of LHD On-Board Monitoring System in a Deep Underground Mine. *Energies* **2023**, *16*, 2149. [CrossRef]
43. Ziętek, B.; Banasiewicz, A.; Zimroz, R.; Szrek, J.; Gola, S. A Portable Environmental Data-Monitoring System for Air Hazard Evaluation in Deep Underground Mines. *Energies* **2020**, *13*, 6331. [CrossRef]
44. Jo, B.; Khan, R. An Internet of Things System for Underground Mine Air Quality Pollutant Prediction Based on Azure Machine Learning. *Sensors* **2018**, *18*, 930. [CrossRef]
45. Nie, W.; Liu, X.; Liu, C.; Guo, L.; Hua, Y. Prediction of dispersion behavior of typical exhaust pollutants from hydraulic support transporters based on numerical simulation. *Environ. Sci. Pollut. Res.* **2022**, *29*, 38110–38125. [CrossRef]
46. Cabaneros, S.M.; Calautit, J.K.; Hughes, B.R. A review of artificial neural network models for ambient air pollution prediction. *Environ. Model. Softw.* **2019**, *119*, 285–304. [CrossRef]
47. Krot, P.; Sliwinski, P.; Zimroz, R.; Gomolla, N. The identification of operational cycles in the monitoring systems of underground vehicles. *Measurement* **2020**, *151*, 107111. [CrossRef]
48. Krot, P.; Zimroz, R.; Sliwinski, P.; Gomolla, N. Safe Operation of Underground Mining Vehicles Based on Cyclic Fatigue Monitoring of Powertrains. In *Structural Integrity and Fatigue Failure Analysis*; Lesiuk, G., Szata, M., Blazejewski, W., Jesus, A.M.d., Correia, J.A., Eds.; Springer: Cham, Switzerland, 2022; pp. 283–292. [CrossRef]
49. Westlund, A. Measuring and Predicting Transient Diesel Engine Emissions. Licentiate Thesis, KTH, School of Industrial Engineering and Management (ITM), Stockholm, Sweden, 2009.
50. Asprion, J.; Chinellato, O.; Guzzella, L. A fast and accurate physics-based model for the NOx emissions of Diesel engines. *Appl. Energy* **2013**, *103*, 221–233. [CrossRef]
51. Perez, E.; Blasco, X.; Garcia-Nieto, S.; Sanchis, J. Diesel engine identification and predictive control using Wiener and Hammerstein models. In Proceedings of the 2006 IEEE Conference on Computer Aided Control System Design, 2006 IEEE International Conference on Control Applications, 2006 IEEE International Symposium on Intelligent Control, Munich, Germany, 4–6 October 2006. [CrossRef]
52. Alcan, G.; Unel, M.; Aran, V.; Yilmaz, M.; Gurel, C.; Koprubasi, K. Diesel Engine NOx Emission Modeling Using a New Experiment Design and Reduced Set of Regressors. *IFAC-PapersOnLine* **2018**, *51*, 168–173. [CrossRef]
53. Hirsch, M.; Alberer, D.; del Re, L. Grey-Box Control Oriented Emissions Models. *IFAC Proc. Vol.* **2008**, *41*, 8514–8519. [CrossRef]
54. Sakushima, N.; Wolf, B.; Karsten, R.; Mirko, K. Transient Modeling of Diesel Engine Emissions. *Int. J. Automot. Eng.* **2013**, *4*, 63–68. [CrossRef]
55. Grahn, M.; Johansson, K.; McKelvey, T. Data-driven emission model structures for diesel engine management system development. *Int. J. Engine Res.* **2014**, *15*, 906–917. [CrossRef]
56. Formentin, S.; Corno, M.; Waschl, H.; Alberer, D.; Savaresi, S.M. Estimation in Diesel Engines via In-Cylinder Pressure Measurement. *IEEE Trans. Control Syst. Technol.* **2014**, *22*, 396–403. [CrossRef]
57. Roy, S.; Banerjee, R.; Bose, P.K. Performance and exhaust emissions prediction of a CRDI assisted single cylinder diesel engine coupled with EGR using artificial neural network. *Appl. Energy* **2014**, *119*, 330–340. [CrossRef]
58. Kakaee, A.H.; Rahnama, P.; Paykani, A.; Mashadi, B. Combining artificial neural network and multi-objective optimization to reduce a heavy-duty diesel engine emissions and fuel consumption. *J. Cent. South Univ.* **2015**, *22*, 4235–4245. [CrossRef]
59. Pillai, R.; Triantopoulos, V.; Berahas, A.S.; Brusstar, M.; Sun, R.; Nevius, T.; Boehman, A.L. Modeling and predicting heavy-duty vehicle engine-out and tailpipe nitrogen oxide (NOx) emissions using deep learning. *Front. Mech. Eng.* **2022**, *8*. [CrossRef] [PubMed]
60. Rubeli, B.; Gangal, M.; Counter, D. The Effects of Depth on Diesel Engine Emissions in an Underground Mine. In Proceedings of the Powertrain & Fluid Systems Conference and Exhibition, Chicago, IL, USA, 29–31 October 2007; SAE International: Warrendale, PA, USA, 2007; pp. 1071–1081. [CrossRef]
61. Asad, U.; Kelly, C.; Wang, M.; Tjong, J. Effects of Intake Air Humidity on the NOX Emissions and Performance of a Light-Duty Diesel Engine. In Proceedings of the ASME 2012 Internal Combustion Engine Division Fall Technical Conference, Vancouver, BC, Canada, 23–26 September 2012; American Society of Mechanical Engineers: New York, NY, USA, 2012; pp. 235–242. [CrossRef]
62. Yuan, Z.; Shi, X.; Jiang, D.; Liang, Y.; Mi, J.; Fan, H. Data-Based Engine Torque and NOx Raw Emission Prediction. *Energies* **2022**, *15*, 4346. [CrossRef]

63. KGHM ZANAM LHD LD1701. 2023. Available online: https://www.kghmzanam.com/wp-content/uploads/2021/05/LKP_1701_EN.pdf (accessed on 16 March 2023).
64. DEUTZ TCD 12.0 and TCD 16.0 Diesel Engine. 2023. Available online: https://www.deutzsupport.com/product-details/tcd-12-0-and-tcd-16-0/ (accessed on 16 March 2023).
65. Funk, S. *Real World NOx Sensor Accuracy Assessment and Implications for REAL NOx Tracking*; SAE Technical Paper Series; SAE International: Warrendale, PA, USA, 2021; p. 9. [CrossRef]
66. Kawamoto, Y.; Todo, Y.; Shimokawa, H.; Aoki, K.; Kawai, M.; Ide, K. Development of High Accuracy NOx Sensor. In *Proceedings of the WCX SAE World Congress Experience, Detroit, MI, USA, 9–11 April 2019*; SAE International: Warrendale, PA, USA, 2019; p. 7. [CrossRef]
67. Iqbal, M.Y.; Wang, T.; Li, G.; Li, S.; Hu, G.; Yang, T.; Gu, F.; Al-Nehari, M. Development and Validation of a Vibration-Based Virtual Sensor for Real-Time Monitoring NOx Emissions of a Diesel Engine. *Machines* **2022**, *10*, 594. [CrossRef]
68. Desai, M.; Shah, M. An anatomization on breast cancer detection and diagnosis employing multi-layer perceptron neural network (MLP) and Convolutional neural network (CNN). *Clin. eHealth* **2021**, *4*, 1–11. [CrossRef]
69. Gaudart, J.; Giusiano, B.; Huiart, L. Comparison of the performance of multi-layer perceptron and linear regression for epidemiological data. *Comput. Stat. Data Anal.* **2004**, *44*, 547–570. [CrossRef]
70. Taud, H.; Mas, J. Multilayer perceptron (MLP). In *Geomatic Approaches for Modeling Land Change Scenarios*; Lecture Notes in Geoinformation and Cartography; Camacho Olmedo, M., Paegelow, M., Mas, J.F., Escobar, F., Eds.; Springer: Cham, Switzerland, 2018; pp. 451–455.
71. Mahmoud, A.A.; Elkatatny, S.; Al Shehri, D. Application of machine learning in evaluation of the static Young's modulus for sandstone formations. *Sustainability* **2020**, *12*, 1880. [CrossRef]
72. Goli, A.; Khademi-Zare, H.; Tavakkoli-Moghaddam, R.; Sadeghieh, A.; Sasanian, M.; Kordestanizadeh, R.M. An integrated approach based on artificial intelligence and novel meta-heuristic algorithms to predict demand for dairy products: A case study. *Netw. Comput. Neural Syst.* **2021**, *32*, 1–35. [CrossRef]
73. Regulation of the Minister of Energy related to operations of underground mining (available in Polish: Rozporzadzenie Ministra Energii z dnia 23 listopada 2016r., w sprawie szczegółowych wymagań dotyczacych prowadzenia ruchu podziemnych zakładów górniczych, Dziennik Ustaw, 1118, 2017. Available online: https://isap.sejm.gov.pl/isap.nsf/DocDetails.xsp?id=WDU20170001118 (accessed on 16 March 2023).